REPORT NO. 4

HYDRAULICS OF SINGLE SPAN ARCH BRIDGE CONSTRICTIONS

MAY 1961

NO. 11

Joint Highway Research Project

PURDUE UNIVERSITY
LAFAYETTE INDIANA

by

P.F. BIERY

J.W. DELLEUR

Report No. 4

Hydraulics of Single Span Arch Bridge Constrictions

by

P. F. Biery
Research Engineer, Johns Manville, Inc., Manville, N.J
formerly Research Assistant, Purdue University

and

J. W. Delleur
Associate Professor of Hydraulic Engineering

State Highway Department of Indiana
in Cooperation with
U.S. Department of Commerce
Bureau of Public Roads

Joint Highway Research Project
Project No. C-36-62B
File No. 9-8-2

Purdue University
School of Civil Engineering
Hydraulic Laboratory

May, 1961

HYDRAULICS OF SINGLE SPAN ARCH BRIDGE CONSTRICTIONS[1]

by F. F. Pilny[2], AM.ASCE and J. W. Delleur[3], M.ASCE

Synopsis

The results of model testing of semicircular arch bridge constrictions are presented. All tests were run for the condition of no skew, no eccentricity and no entrance rounding. A generalized backwater equation is presented, by means of which one can evaluate the backwater superelevation in terms of the bridge span, the stream width and the Froude number of the approach flow. The equation holds for geometries other than semicircular constrictions. Design procedures for indirect discharge measurement, for determination of backwater superelevation, and for determination of required waterway area are given. A model-prototype comparison is discussed.

---

1 - Presented at the national ASCE convention, Hydraulic Division, Hydraulic Structures Session, October 14, 1960

2 - Research Engineer, Johns Manville, Inc., Manville, New Jersey, formerly Research Assistant, School of Civil Engineering, Purdue University

3 - Associate Professor of Hydraulic Engineering, School of Civil Engineering, Purdue University, Lafayette, Indiana

INTRODUCTION

In recent years, the problem of protecting the flood plains from flood damage has become increasingly important. In order to eliminate or minimize any additional flood effects, the highway engineer must be able to predict the influence of a new highway bridge upon stream stage during high flood flows. It is generally recognized that the construction of a bridge is going interfere with the natural flow of the stream and results in a rise in stage upstream and an increase in velocity through the bridge. It is the highway engineer's responsibility to provide the minimum span length for structural and economic reasons, and yet to allow a large enough water area to keep the rise in backwater within tolerable limits. Without the necessary information to make an intelligent estimate of the maximum backwater, overdesign or underdesign results in making either the cost of the bridge prohibitive or the risk of flood damage excessive.

In the past, studies by the U. S. Geological Survey and the Bureau of Public Roads pertaining to the backwater effects caused by bridge constrictions have considered shapes of openings such as those produced by straight deck bridges. However, very little has been done in the way of making a systematic study of the hydraulics of river flow under the various shapes of arch bridges. The arch is unique in that the surface width of the water surface within the barrel of the arch decreases with a corresponding increase in stage.

A project was initiated in the Hydraulics Laboratory at Purdue University to study the hydraulics of stream flow under arch bridges. It is sponsored by the Indiana State Highway Department in cooperation with

the U. S. Bureau of Public Roads. The purpose of this research is to study the hydraulics of arch bridge constrictions and to provide a method for computing the backwater upstream of the bridge.

The earliest systematic laboratory investigation of flow through contractions in open channels was performed by E. W. Lane.[1]* He related the discharge and the water surface elevation through the contraction by means of empirical discharge coefficients, and indicated that there may exist some relationship between these coefficients and the ratio of the maximum backwater depth produced by the contraction to the normal depth of flow without the contraction. This ratio is referred to as the backwater ratio.

In 1945, Kindsvater and Carter[2] presented a practical solution to the discharge problem by an extensive experimental investigation. By applying correction terms for various geometric conditions to a standard discharge coefficient, the method can be applied to a wide variety of boundary conditions. A detailed description of the internal and external flow characteristics was given.

In the same year, R. S. Bundy and R. W. Carter[3] presented a companion paper to the one by Kindsvater and Carter. In it they gave a method of computing the nominal backwater due to open channel constrictions. The practical solution was based upon empirical discharge coefficients and a laboratory investigation of the influence of channel roughness, channel shape, and constriction geometry. Their study was limited to single span, dock type constrictions and to steady tranquil flow. C. F. Izzard,[4] in his discussion of this paper, pointed out that the backwater ratio expressed as y_1/y_n (see Figure 1) is a function of the normal depth

* Superscripts refer to references in the bibliography.

Based upon the model tests conducted at Colorado State University, J. N. Bradley[7] compiled a report entitled "Hydraulics of Bridge Waterways". The publication was completed in August 1960 and is the first in a series of reports on the hydraulic design of highway drainage structures. This

particular report, within limitations, is intended to provide a means of computing the effect of a given bridge upon the flow in a stream.

H. R. Vallentine[8] reports on tests performed to study the characteristics of flow in a rectangular channel with symmetrically placed sharp edged constriction plates placed normal to the flow. The flow is related to the upstream depth by means of a weir type discharge equation. The experimental coefficients were found to depend upon the geometry of the constriction and the Froude number of the approaching flow. The conditions which produce an increase in the upstream depth were investigated and the extent of the increase evaluated.

Some recent work done at Lehigh University[9] tells about the effects of placing spur dikes on the upstream side of a bridge constraction. These dikes are designed to increase the hydraulic efficiency of the bridge crossing by lowering the backwater curve and reducing the velocity underneath the bridge. This particular report presents a good qualitative description of the flow patterns through the bridge constriction.

A preliminary investigation including some model testing of semi-circular arch constrictions was done at Purdue university by Chen, Scoby, Hueds and Collins[10] in 1958 and 1959. The backwater superelevation was related to the Froude number of the approaching flow and to the ratio of the arch span to the stream width. The present paper is an outgrowth of this preliminary study.

The area of the arch segment ideal is

$$A_{n2} = \int_0^{y_n} 2\sqrt{r^2 - y^2}\, dy = \int_{\theta_1}^{\pi} 2r\sin^2\theta\, d\theta \qquad \text{---(9)}$$

and the corresponding channel opening ratio is

$$M' = A_{n2}/A_{n1} = \frac{2\int_{y_n}^{r}\sqrt{r^2 - y^2}\, dy}{\int_{y_n}^{r} 2y\, dy} = \frac{\int_{\theta_1}^{\pi} r^2\sin^2\theta\, d\theta}{\int_{y_n}^{r} 2y\, dy} \qquad \text{---(10)}$$

The channel opening ratio M' can be expressed in terms of three dimensionless ratios, two of which are the normal depth to the rise ratio $\eta = y_n/b$, the ratio of depth of the arch crown below the crown tangent to the rise ratio $\zeta = d/b$ and the ratio of normal depth to arch radius $\xi = y_n/r$. The channel opening ratio of equation (10) may then be expressed as:

$$M' = \frac{A_{n2}}{A_{n1}} \qquad \text{---(11)}$$

where

$$A_{n1} = \eta b^2$$

and

$$\frac{A_{n2}}{A_{n1}} = 1/2\left[\frac{\cos^{-1}(1-\xi) - (1-\xi)\sqrt{2\xi - \xi^2}}{\eta\left(\frac{b}{r}\right)^2}\right] - \left[\frac{\sqrt{1-\eta^2} - \cos^{-1}\eta}{\eta\sqrt{1-\eta^2}}\right] \qquad \text{---(12)}$$

which

$$\eta = y_n/b$$

and

$$\xi = y_n/r$$

In the form of equation (11) the value of $M = b/B$ is adjusted for the particular arch by an amount equivalent to ζ_1 such that M' is the ratio of A_{n2} to A_{n1}. In the more general case, the values of ζ and η can take on numbers within certain limits, before the normal depth will submerge the crown of the arch. The limits are as follows:

For $\eta = y_n/r$ $\quad 0/r \le y_n/r \le (r - \zeta r)/r$ $\qquad$ ---(13)

or

$$0 \leq \zeta \leq (1 - \gamma)$$

for $\gamma = d/r \quad 0 \leq \gamma \leq 1$

When $\gamma = 0$, the case of a semicircular arch with the center of curvature at the springline exists. When $\gamma = 1$, the contraction reduces to two parallel abutments.

The values of C_M have been calculated for several values of ζ and γ and are given in the graph of Figure 3. The submergence limit represents the upper limits of both ζ and γ. The segment arch which is a constant radius arch with the center of curvature below the springline of the arch (that is $\gamma > 0$) can be used as an arch in its own right or as an approximation to an elliptical or a multiple radius arch. The value of M' for the elliptic and multiple radius arch could be determined directly from equation (7). However, they have not been worked out in the present research. If equation (13) were applied to vertical abutment bridge piers as idealized in Fig. 2a, 2b, the value of C_M would become unity.

An approximate form of the equation for the discharge through a two dimensional semicircular arch constriction in a rectangular channel may be expressed in terms of an infinite series of powers of the y_1/r. With reference to figure 1, the Bernoulli theorem gives;

$$Q = \int V \, dA = \int_0^{y_1} C_d \sqrt{2g(y_1 - h)} \times 2\sqrt{r^2 - h^2} \, dh \qquad \text{---(14)}$$

Expanding equation (14) into a series and integrating term by term and making use of the fact that $2r = b$;

$$Q = C_d \sqrt{2g} \; 17/24 \; y_1^{3/2} b \left[1 - 0.1294(y_1/r)^2 - 0.0177(y_1/r)^4 \right] \qquad \text{---(15)}$$

This may be written as

$$Q = C_y y_1^{3/2} b \; \mathcal{F} \qquad \text{---(16)}$$

where $\mathcal{F} = C_d \; 17/24 \sqrt{2g} \qquad \text{---(17)}$

and $$\quad = \left[\left(1 - 0.12\left(y_1/x\right)^2 - 0.\ldots\right)\right] \qquad \text{---(18)}$$

The discharge in a rectangular approach channel may also be expressed by

$$Q = V_n A_n = F_n \sqrt{g}\ b\ y_n^{3/2} \qquad \text{---(19)}$$

where $$F_n = V_n / \sqrt{g\ y_n}$$

is the Froude number of the undisturbed normal depth flow. Equating (15) and (19) and solving for the discharge coefficient

$$C_d = \left(12\sqrt{2}\ \ \ / 17\ \ N^2\right)\left(y_n / y_1\right)^{3/2} \qquad \text{---(20)}$$

Typical values of the coefficient of discharge C_d are shown in figure 8 which shows the results of the two dimensional semi-circular arch tests in the rectangular channel. It is interesting to note the limiting condition of the discharge coefficient as M^1 goes from zero to one. For a two dimensional ideal orifice, Streeter[12] shows that the application of the theory of free streamlines leads to an ideal discharge coefficient of

$$\left(\frac{2b}{\pi}\right)_{\frac{2b}{\pi}} = \pi/(\pi + 2) = 0.611 \qquad \text{---(21)}$$

The coefficients of discharge curves of figure 8 converge to 0.611 showing that this is a limiting value of C_d as M^1 approaches zero.

When M is equal to unity, $C_d = 1$ and $b/B = 1$. Therefore, $b = B$ and there is no contraction at all. If there is no contraction, then $y_1/y_n = 1$ and $I = 1$. Also $12\sqrt{2} / 17 = 0.9981$ which is approximately unity. Therefore equation (20) becomes

$$\text{at } M^1 = 1 \qquad 1 = \left(F_n / C_d \right)^{2/3}$$

Therefore as the opening ratio tends to unity, the discharge coefficient tends to the Froude number of the undisturbed flow.

The Backwater Ratio Equation

The backwater ratio is defined as the ratio of the maximum centerline water depth to the normal depth of flow. Since M = M'/C equation (20) may be rearranged such that the backwater ratio becomes

$$y_1/y_n = (12\sqrt{2}\ F_r\ /\ 17\ C_d\ M')^{2/3} \qquad \text{---(23)}$$

It has been observed that the equations derived by several different investigators for the backwater ratio produced by various constriction geometries seem to have a basic similarity. As an example, equation (23) in the present text for y_1/y_n appears to be a function of $(F_n/M')^{2/3}$.

$$y_1/y_n = g_1(F_n/M')^{1/3} \qquad \text{---(24)}$$

An equation for the backwater ratio given by Valentine[6] for natural constriction plates is

$$y_1/y_n = (g\ F_n/C\ H)^{2/3} = g_2(F_n/M')^{2/3} \qquad \text{---(25)}$$

Also Iida[6] presents an empirical formula for a two dimensional vertical board model.

$$(h_1^*/h_n)^3 = 4.1\sqrt{2}\ F_n^2\ (\tfrac{1}{M'^2} - \tfrac{2}{3}(2.5 - M)) = 1 \qquad \text{---(26)}$$

Considering only the leading term F_n/M'^2 of the quantity in brackets, equation (26) becomes

$$h_1^*/h_n = g_3\ (F_n/M')^{2/3} \qquad \text{---(27)}$$

Therefore it appears possible that with the proper interpretation of the variables, namely M' and F_n, the results of tests performed on different geometric shapes of bridge openings may produce the same results. For instance, a vertical abutment deck type bridge may physically appear completely different from a semicircular arch bridge. However, for hydraulic considerations, if they have the same opening ratio M', they may produce the same backwater ratio. The limitations of the assumption must necessarily lie in the fact that both bridges must have the same

eccentricity, closeness and arterial rounding conditions. It is believed that this concept applies equally as well to multiple span bridges. An attempt has been made to compare the two dimensional semicircular test results the segment data, and the Vertical Board (VB) data as given by Liu[6]. The results of this comparison in Figure 14 have substantiated the assumption of the similarity between the functions g_1, g_2 and g_3.

EXPERIMENTAL EQUIPMENT

Small Flume and Models

For the purpose of preliminary testing, a small variable slope flume 6" wide and 12' long was used. The channel sides and bottom were constructed of lucite and carefully aligned by means of adjusting screws. The slope of the flume was controlled by a hand operated scissor jack at the lower end of the flume. An aluminum I-beam mounted horizontally above the flume served as a track for the mechanical and electric point gages used in obtaining the water surface measurements. The flow was metered by a 1 inch orifice plate in a 2 inch supply line. Two and three dimensional models were tested with both smooth and rough boundaries. For the rough boundary tests, the bottom and the walls were lined with copper wire mesh of 14 meshes per inch.

The two dimensional semicircular models were constructed with diameters of 3, 4, and 5 inches. The material used was brass. The edges were machined to 1/32 of an inch and then beveled to a 45 degree angle. The two dimensional segment models were of the same type of construction as the semicircular models and had a value of $\eta = d/r$ equal to 0.5 (see Figure 2b). The three dimensional semicircular models for the small flume were made of clear lucite. The length for all three dimensional models was 24 inches. The testing of segment arches was limited to the small flume only.

Large Flume and Models

The majority of the tests reported here were performed in a larger 2 foot by 5 foot by 64 foot all steel tilting flume. The slope was controlled by six screw jacks driven by a common motor and gear reducer. The motor was operated by a raise, lower and stop switch. A revolution counter was attached at one end of the drive shaft and the actual slope of the flume bed was related to the number of revolutions and tenths of revolutions of the shaft. In this manner a change of slope with an accuracy of $\pm$ 0.000025 feet/foot was easily accomplished in a matter of minutes. An 8 foot by 10 foot head box was equipped with an elliptical transition to provide a smooth change as the water flowed into the flume. The head box also contained several screens and one larger stone baffle. A skimming board which floated on the water surface prevented the propagation of surface waves in the flume. At the discharge end of the flume an adjustable sharp crested rectangular weir made of lucite was installed. A catchment box was made to eliminate any splash. The box discharged directly to the sump. The water was taken from a large recirculatory sump. One 2000 GPM pump and one 300 GPM pump fed the head box. The actual inflow was metered by two venturi's. The layout of the flume and the water supply system is shown in Figure 4.

An aluminum instrument carriage was mounted on adjustable stainless steel guide rails running the length of the flume. It was installed in such a manner that the flume bottom could be used as a reference plane. On the rack were mounted an electric point gage and a 1/4 inch Prandtl tube. The staff of the point gage was marked in millimeters and was equipped with a vernier which read to a tenth of a millimeter. The Prandtl tube was the type used normally for air. It was connected to an inverted U manometer which had a fluid of specific gravity 0.810. In addition a 50-tube piezometer stand was installed to obtain rapid

measurement of the surface pressure. Fifty pressure taps located at points along two centerlines and 1 ft., and 2 ft. right and left of the centerline were hooked up to the piezometer tubes. The bank was constructed so that it could be tilted to a 4:1 longitudinal slope and was illuminated from the inside.

Sixteen models were used in the testing program. They were designed for specific values of L/B and L/b, where L is the length of the model measured in the direction of the flow. For a relative length ratio of L/b = 0, four models were tested, one for each of the following values of M = b/B, M = 0.3, 0.5, 0.7, and 0.9. They were constructed with 1/2 inch marine plywood and lined with 22 gage galvanized sheet metal. The three dimensional models had height width values of 0.3, 0.5, 0.7, and 0.9. In each group two models were constructed with L/b = 0.25 and one model with L/b = 0.5. The main construction was 1/2 inch marine plywood. The barrel was formed with galvanized sheet metal and one side of one of the L/b = 0.25 models was faced with lucite. Figure 5 illustrates the three dimensional bridge models. Shown are the four models with L/b = 0.25 and M = 0.3, 0.5, 0.7, and 0.9. With this combination of models it was possible to test each of the openings M = 0.3, 0.5, 0.7, and 0.9 for relative lengths L/b of 0, 0.25, 0.50, 0.75, and 1.00. All of the models tested in the large flume were either two or three dimensional semi-circular models. The testing section was located between 20 and 50 feet from the entrance where it was possible to maintain uniform flow. In all cases the regain curve between sections 3 and 4 (Figure 1) was within the test section. In the great majority of the cases the boundary layer was fully developed within the first 20 feet of the flume, and fully developed uniform flow existed in the test section.

The actual testing program in the large flume was run under two different boundary roughness [illegible]

referred to as the smooth boundary consisted of the tilting flume walls being finished with an epoxy resin paint.

Manning's n for smooth boundaries had an average value of 0.0110. The range of n varied from 0.009 to 0.013 for discharges and Froude numbers from 1 cfs to 4 cfs and 0.05 to 1.00 respectively.

For the rough boundaries, the following roughness pattern was selected. Along the bottom of the flume, two layers of 1/4 inch aluminum rods were placed in a square pattern with longitudinal bars placed 12 inches on center, and a top layer of the same bars 6 inches on center. Along the sidewalls one layer of similar bars 6 inches on center was placed 1/4 inch from the wall. The bottom layers of bars were tied together with wire. The sidewall bars were tied at the bottom to the transverse bars and placed so that 1/2 above the free surface. The value of Manning's n for the rough boundary ranged from 0.022 to 0.025 for discharges from 1 to 4 cfs and slopes from 0.00030 to 0.00450. The average value of n of 72 uniform flow tests was 0.0238.

Tests

Seventy tests were run in the large flume with smooth boundaries covering a range of discharges from 1 to 2.5 cfs and a channel width ratio M varying from 0.3 to 0.9. One hundred and sixty eight tests were made in the large flume with rough boundaries for the conditions summarized in the table below, where the X's indicate the selected normal depth conditions for each of which the following values of M and L/b:

For M = b/B = 0.3, 0.5, 0.7, 0.9

and L/b = 0.0, 0.5, 1.0

Flow Rate	Froude Number													
	0.05	0.10	0.15	0.20	0.25	0.30	0.35	0.40	0.45	0.50	0.60	0.70	0.80	0.90
1 cfs	X			X		X		X		X		X		
2 cfs		X			X		X		X		X		X	
3 cfs			X											

Also with rough boundaries additional tests were made to establish that the expansion of the flow downstream from the minimum depth (profile between points 3 and 4 of Figure b) was complete and within the limits of the test section. A detailed surface topography was measured for Q = 1 cfs, slope = 0.00584, M = 0.5 and L/b = 0. Sufficient velocity profiles were taken at these conditions to plot isovel diagrams for the sections of uniform depth, maximum depth, vena contracta and the minimum depth. The isoval diagrams were also obtained for uniform flow corresponding to the following conditions:

Q = 1 cfs; slope = 0.004080

Q = 2 cfs; slope = 0.000131

The particular measurements that were taken on each of the smooth and rough boundary tests in the large flume were those required to calculate the following quantities: the hydraulic radius, the Reynolds number, the Froude number, the Darcy-Weisbach friction factor, the channel opening ratio M', the discharge coefficient, the backwater ratio (y_1/y_n), the backwater superelevation (h^*_1), the surface profile ratio ($h^*_1/\Delta h$), the length to the maximum backwater (L_{1-2}), the length to the point of minimum depth (L_{2-3}), the length L_{1-3}, and Manning's n. (See Figure 1 for the definition of terms). In view of the large amount of data that was to be analyzed and the repetitive character of the calculations, a program was prepared for processing the data on the Royal McBee LGP-30 digital computer.

The tabulation of the test data may be found in reference (17)**.

ANALYSIS OF TEST RESULTS

Large Flume Smooth Boundary Model Tests

The experimental results of the two dimensional, semicircular, arch model tests in the large flume with smooth boundaries were plotted

** A copy has been deposited at the Engineering Societies Libraries

as the ba[illegible] ratio y_1/y_2, the channel [illegible], and [illegible]
normal-depth Froude number F_n is the parameter. This [illegible]
figure (as [illegible] explained, the [illegible] of y_1/y_n [illegible] normal
Froude number [illegible] the value [illegible] approaches [illegible], the [illegible]
of decrease [illegible] a similar manner the discharge coefficient [illegible]
plotted vs. F' for [illegible], and [illegible] in Figure 8. [illegible]
(hydraulic jump), [illegible] of y_1 [illegible] to 1.0 [illegible]
approaches the [illegible] value [illegible] vs. F'. [illegible]
of Figure 8 are [illegible] interpolation. [illegible]
The data were plotted [illegible] and [illegible] the [illegible]
curves [illegible] which [illegible] were [illegible] and [illegible]
interpolated [illegible] the [illegible] curves. [illegible]
obtain [illegible] for [illegible] numbers [illegible]
parameter.

[illegible] Flow [illegible]

[illegible] and Discharge Coefficient

[illegible] ratio of [illegible] to channel [illegible] is
[illegible] normal-depth Froude number [illegible] parameter for the [illegible] dimensional
sediment-[illegible] models [illegible] in the range [illegible] rough
boundaries. In view of the importance of [illegible] curves, the scale was
expanded and the results are plotted in two parts. Figure 7a gives the
results of y_1/y_n vs. F' for the range of backwater ratios less than 1.50.
For the ratios greater than 1.50, Figure 7b should be used.

The experimental values of the discharge coefficient for the same test conditions are presented in Figure 8. This figure and Figures 7a and 7b have also been interpolated for constant Froude numbers.

a very reliable estimate of y_2/y_c. In order to [illegible] F_3 vs F_n [illegible] is shown in Figure 10. [illegible] was good. However, above $F_n = 0.5$ the depth [illegible] critical depth and the correlation of F_3/F_n [illegible] was very poor. The author wanted to [illegible] the [illegible] the test results for $F_n = 0.5$ [illegible]. If [illegible] from this curve [illegible]

Comparison of Roughness Effects

Comparisons between [illegible] channel were made by plotting the backwater [illegible] coefficient against the [illegible] Froude number, F_n, for both channel conditions.

It appeared that the [illegible] essentially the same for both smooth and rough conditions [illegible] F_n less than 0.5. Above the practical range of [illegible] channels is that [illegible] than 0.5, there [illegible] for all practical purposes the effect of roughness can be ignored.

Comparison of Bridge Length Effects

Similarly, all of the [illegible] were compared at constant values of the channel opening ratio, M'. Again it appears from the plots that, for the practical range of field conditions, ($I_1 \leq 1.0$ and $F_n \leq 0.5$) the effect of bridge length is negligible. The effect of length did seem to increase with a decrease in the channel opening ratio. However, as the value of M' gets small, the physical properties are closer to those of a culvert rather than a bridge opening.

checked [illegible] analyzed with the [illegible] method [illegible].

In addition [illegible] were obtained [illegible] flow conditions. From these [illegible] Figure 2-6, the following values of the [illegible] correction factor were determined for uniform flow [illegible]:

Q	[illegible]	[illegible]	[illegible]	[illegible]	ξ
2 cfs	[illegible]	[illegible]	[illegible]	[illegible]	1.055
1 cfs	[illegible]	[illegible]	[illegible]	[illegible]	1.045
1 cfs	[illegible]	[illegible]	[illegible]	[illegible]	1.05

Based upon [illegible] the value of [illegible] 1.04. From [illegible], based on [illegible] two dimensional [illegible], [illegible] 1.2 [illegible] from the [illegible] of the [illegible] to take into account the effects of [illegible] and contraction. Other investigators have assumed that [illegible] is unity [illegible] rigid rectangular flumes. This calculation verifies that this assumption [illegible] two dimensional.

THE [illegible] BAKHMETEFF EQUATION

With the introduction of the [illegible] opening ratio M', the assumption was made that [illegible] by constrictions of the same M' would be equal regardless of the physical geometry of the actual constrictions. In order to verify this assumption, tests on a [illegible] geometric shape than a semi-circle were needed.

A series of 9 tests were run by [illegible] A. Seeley in the small flume on two dimensional segment weirs with a $\eta = d/r$ value of 0.5. (see Figure 2). The data obtained were analyzed in terms of M'. These tests were run in the small channel with rough boundaries which had a Manning's n of 0.013. Results were plotted in the same manner as for the large flume

rough tests and are shown in Figure 13. When compared to the same line results of Figure 7, the values of the roughness ratio for a [illegible] and M were almost [illegible] of the [illegible] set of waves had been [illegible] by [illegible] could be attributed to experimental [illegible]

[illegible] by Liu[5] was [illegible] [illegible] were [illegible] their roughness reduced [illegible] the [illegible] circular disk [illegible] were extremely [illegible] [illegible] Its [illegible] extremely [illegible] [illegible] investigators in three [illegible] [illegible] geometries [illegible] [illegible] clearly verified that the channel [illegible] [illegible] were [illegible] [illegible] Of course, the [illegible] was zero, and the [illegible] was zero, and the [illegible]

[illegible] the [illegible] of the results they should have [illegible] the [illegible] ratio y_1/y_n, the [illegible] number F_n and the [illegible] which would fit all or the data. This relationship would then be applicable to all constriction geometries [illegible] previously [illegible] analysis, a similarity was noticed between the several different backwater equations. The term $(F_n/M^2)^{2/3}$ appeared in all of the solutions of y_1/y_n. In general, it appeared that

$$y_1 / y_n = C \left[\left(F_n / M^2 \right)^{2/3} \right]^{\delta} \qquad \text{---(28)}$$

MODEL PROTOTYPE COMPARISON [illegible]

The [illegible] are the normal [illegible] As defined, [illegible] the boundary roughness and the [illegible] relatively [illegible] be neglected [illegible] in defining [illegible] irregular [illegible] irregular natural channel [illegible] A_n/P_n, where [illegible] are [illegible] in the uniform [illegible]

[illegible] (31)

For [illegible]

[illegible] (32)

[illegible] needed. [illegible] number, [illegible] assumed [illegible] factor [illegible] field [illegible] could [illegible] the differences between model and prototype. This [illegible] similarity it is necessary that

$$\left(V / \sqrt{g\, y_n / \alpha} \right)_{model} = \left(\sqrt{Q^2\, y_n / A_n^3\, g / \alpha} \right)_{prototype}$$

or

$$\left(V / \sqrt{g\, y_n} \right)_{model} = \left(\sqrt{Q^2\, y_n / A_n^3\, g} \right)_{prototype} \sqrt{\alpha_p / \alpha_m} \qquad (33)$$

3.) With this [illegible] and [illegible] at surface 4 [illegible]
Plot the [illegible] on the [illegible] Figure 15.

B. Trial and Error [illegible] for [illegible]

1.) [illegible] the [illegible] Table the maximum
[illegible] for the given [illegible]

2.) Enter [illegible] with this [illegible] and obtain the maximum
[illegible] from [illegible]

3.) [illegible] and [illegible]
[illegible]

4.) [illegible] the [illegible] hydraulic depth [illegible]

5.) [illegible] the [illegible] normal depth [illegible] with
[illegible]

6.) [illegible] obtain the corresponding
[illegible]

7.) [illegible] the [illegible] opening
[illegible] approach area A_{n1}
[illegible] and (1) respectively.

8.) [illegible] check the normal depth Froude number
from equation (27).

9.) With the Froude number F_{n1} derived to equation (32), calculate
the discharge Q. This will give a first estimate of the
flood [illegible]

10.) With F and F_{n1} go to Figure 3 and obtain the discharge
coefficient C_d.

11.) As a second estimate, compute the discharge according to
equation (15), where b is the distance between abutments at
the springline of the arch, r is the radius of curvature
of the [illegible] and [illegible] from the maximum [illegible]

4.) Calculate y_0/s and obtain the value of C_y from figure 5 for the curve of $\eta = 0$. When the center of curvature

CONCLUSION

ACKNOWLEDGMENT

This research was sponsored by the State Highway Department of Indiana in cooperation with the U. S. Department of Commerce, Bureau of Public Roads. The author gratefully acknowledges his appreciation to Mr. D. P. Izzard, Director of Hydraulic Research, U. S. Bureau of Public Roads, Washington, D. C. for his helpful comments and suggestions and to Mr. H. J. Owen, Executive Secretary, Illinois Water Resources Commission, Urbana, Illinois for his research Assistant at Purdue University, designed and supervised the construction of the large flume and started the model testing. Thanks are also given to Mr. A. A. Scorgie, Research Engineer, Purdue University, who performed the testing of negative and [illegible] flows.

BIBLIOGRAPHY

1. Lane, E. W. "Experiments on the Flow of Water Through Contractions in Open Channels", Trans. ASCE, Vol [illegible], 1910-20 pp. 1249-1219

2. Kindsvater, C. E. and Carter, R. W. "Tranquil Flow through Open-Channel Constrictions", Trans. ASCE, Vol. 120, 1955, pp. 955-980

3. Tracy, H. J. and Carter, R. W. "Backwater Effects of Open-Channel Constrictions", Trans. ASCE, Vol. 120, 1955, pp. 993-1006

4. Izzard, C. F. Discussion on "Backwater Effects of Open-Channel Constrictions" by H. J. Tracy and R. W. Carter, Trans. ASCE, Vol. 120, 1955, pp. 1008-1013

5. Kindsvater, C. E., Carter, R. W. and Tracy, H. J. "Computation of Peak Discharge at Contractions", U.S.G.S. Circ. #284, Washington, D. C., 1953.

6. Liu, H. K., Bradley, J. N. and Plate, E. J. "Backwater Effects of Piers and Abutments", Colorado State University, CER57HKL10, October, 1957

7. Bradley, J. N. "Hydraulics of Bridge Waterways", U. S. Department of Commerce, Bureau of Public Roads, Washington, D. C., August 1960

8. Valentine, H. R. "Flow in Rectangular Channels with Lateral Constriction Plates", La Houille Blanche, Jan.-Feb. 1958, pp. 73-84.

9. Rehbock, J. F., Carter, R. J. and Kable, J. C. "The Effects of Spur Dikes on Flood Flow Through Highway Bridge Constrictions", Fritz Engineering Laboratory, Lehigh University, June, 1959.

10. Owen, H. J., Dooky, A. A., Hussain, S. T., and Delleur, J. W. "Hydraulics of River Flow Under Arch Bridges - A Progress Report", Proceedings of the 4th Road School, Purdue Engineering Experiment Station, Series No. 100, March 1960.

11. Buckingham, E. "On Physically Similar Systems", Phys. Rev., Vol. 4, Ser. 2, pp. 345-376, 1931

12. Streeter, V. L. "Fluid Dynamics", McGraw-Hill Book Co., New York, 1948, pp. 174-177.

13. Owen, H. J. "Design and Construction of a Hydraulic Testing Flume and Backwater Effects of Semicircular Constrictions in a Smooth Rectangular Channel", Progress Report No. 2, Joint Highway Research Project, Purdue University, January, 1960.

14. Daugherty, R. L. and Ingersoll, A. C. "Fluid Mechanics", McGraw-Hill Book Co., New York, 1954.

15. Chow, V. T. [illegible] Hydraulics [illegible] McGraw-Hill [illegible], New York, 1959

16. Henry, H. [illegible] [illegible] [illegible] by Anderson, Hal, Fountain, [illegible] [illegible] Vol II, 1950, pp. 687-694

17 Biery [illegible] Delta [illegible] Open Arch Bridge Constriction [illegible] Report [illegible] Project No. C-3(6)-[illegible] [illegible] [illegible] Bridge, Indiana

NOTATIONS

SYMBOL	UNIT	DEFINITION
A	L^2	Area
A_{n1}	L^2	Flow area at section 1
A_{n2}	L^2	Flow area at section 2
a	L	Throat length
B	L	Top width of flow area in a curved or non-rectangular channel
b	L	Bottom width of a channel or springline of the arch
C		Coefficient
C	$L^{1/2}/T$	Conveyance coefficient = $\frac{1.486}{n} R_n^{2/3}$
C_d		Coefficient of discharge
C_E		Energy ratio coefficient
D	L	Flow depth as defined by V. T. Chow
d	L	Flow depth in a deep open channel
d_c	L	Critical depth from the springline to the center of curvature of the arch
F		Denotes a mathematical function
F_n		Froude depth Froude number = $V_1/\sqrt{gy_n}$
F_3		Froude number at the section of minimum depth
f		Denotes a mathematical function
f		Darcy-Weisbach friction factor
G		Denotes a mathematical function
g		Denotes a mathematical function
g	L/T^2	Acceleration of gravity
H	L	Total energy head

n_1^*	L	Ma[illegible] suction [illegible]tion
h	L	L[illegible] [illegible]e ma[illegible] [illegible]
[illegible]		[illegible] [illegible] [illegible]
[illegible]		[illegible]
[illegible]		[illegible]
L_{a-2}		[illegible] the [illegible]
[illegible]		[illegible]
[illegible]		b/B
[illegible]		[illegible]
N_1		[illegible] [illegible] open channel
[illegible]	$L^{1/6}$	[illegible] [illegible]
[illegible]		[illegible] [illegible]
p	L^3	[illegible]
Q	L^3/T	[illegible]
q	$L^3/$[illegible]	[illegible] [illegible]
R	L	Hydraulic radius
r	L	Radius of curvature of the arch
S		Slope
[illegible]		An infinite series of powers of the ratio of the maximum depth to the radius of curvature

V	L/T	Average velocity
v	L/T	Local velocity
y	L	Depth of flow
y_n	L	Depth of the normal unconstricted flow
y	L	Depth of flow at the section of maximum backwater
y_2	L	Depth of flow at the vena contracta
y_3	L	Minimum depth of flow
α		Kinetic energy coefficient
β		Momentum coefficient
γ	F/L^3	Specific weight of water
ζ		Ratio of y_n / r
		Ratio of d / r
ν	L^2/T	Kinematic viscosity of the fluid
ρ	FT^2/L^4	Fluid mass density

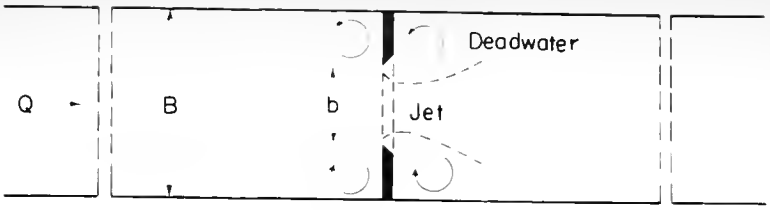

A.) PLAN

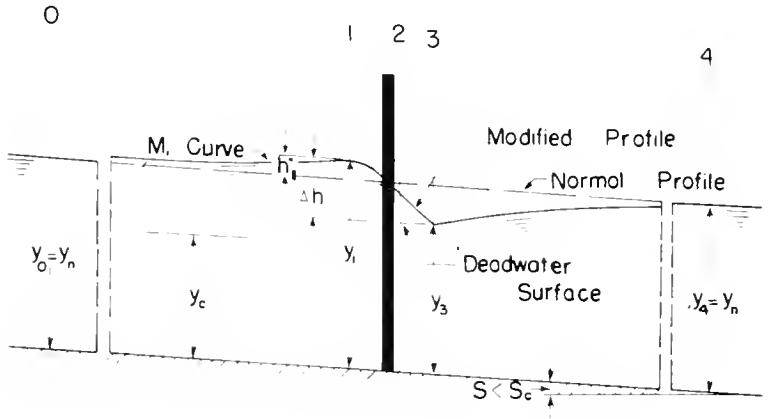

B) MILD SLOPE CHANNEL

C.) WEIR PLATES

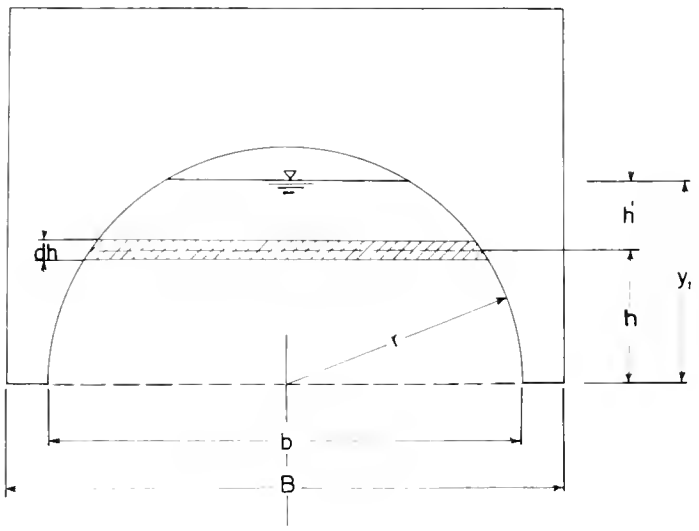

FIGURE 1 DEFINITION SKETCH

(a)

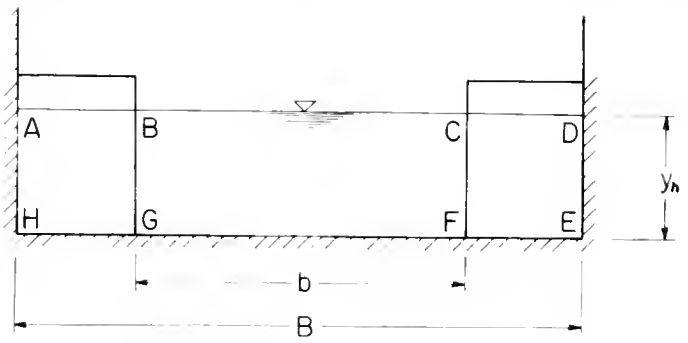

FLOW IN ADEH = $Q = V_n B y_n$

FLOW IN BCFG = $q = V_n b y_n$

(b)

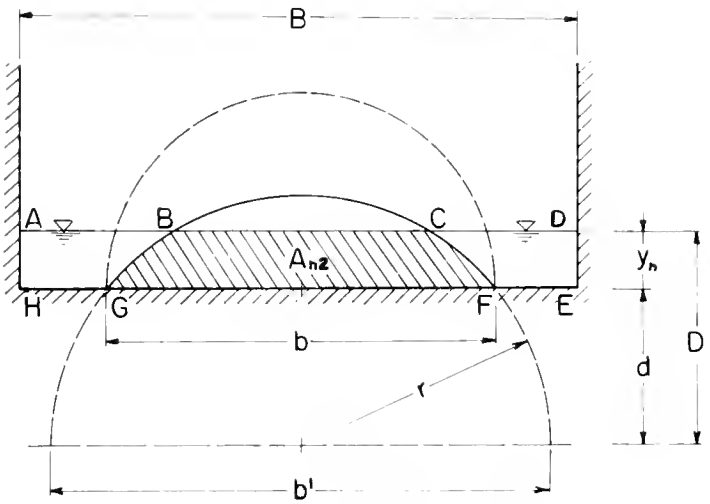

FLOW IN ADEH = $Q = V_n B y_n$

FLOW IN BCFG = $q \neq V_n b y_n$

FIGURE 2 — DEFINITION SKETCH FOR THE DEVELOPMENT OF THE CHANNEL OPENING RATIO

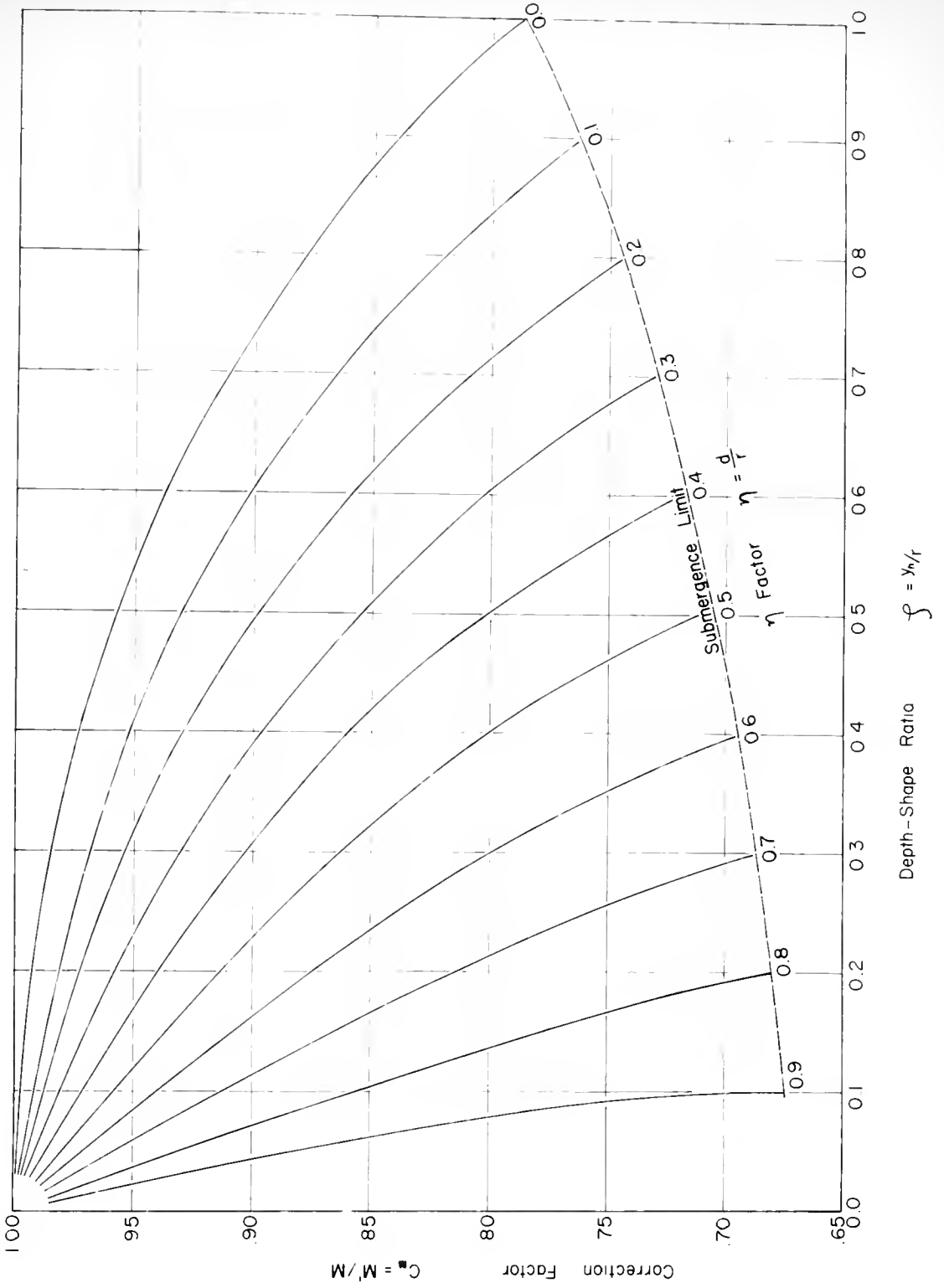

FIGURE 3 — CORRECTION COEFFICIENT FOR THE CHANNEL OPENING RATIO

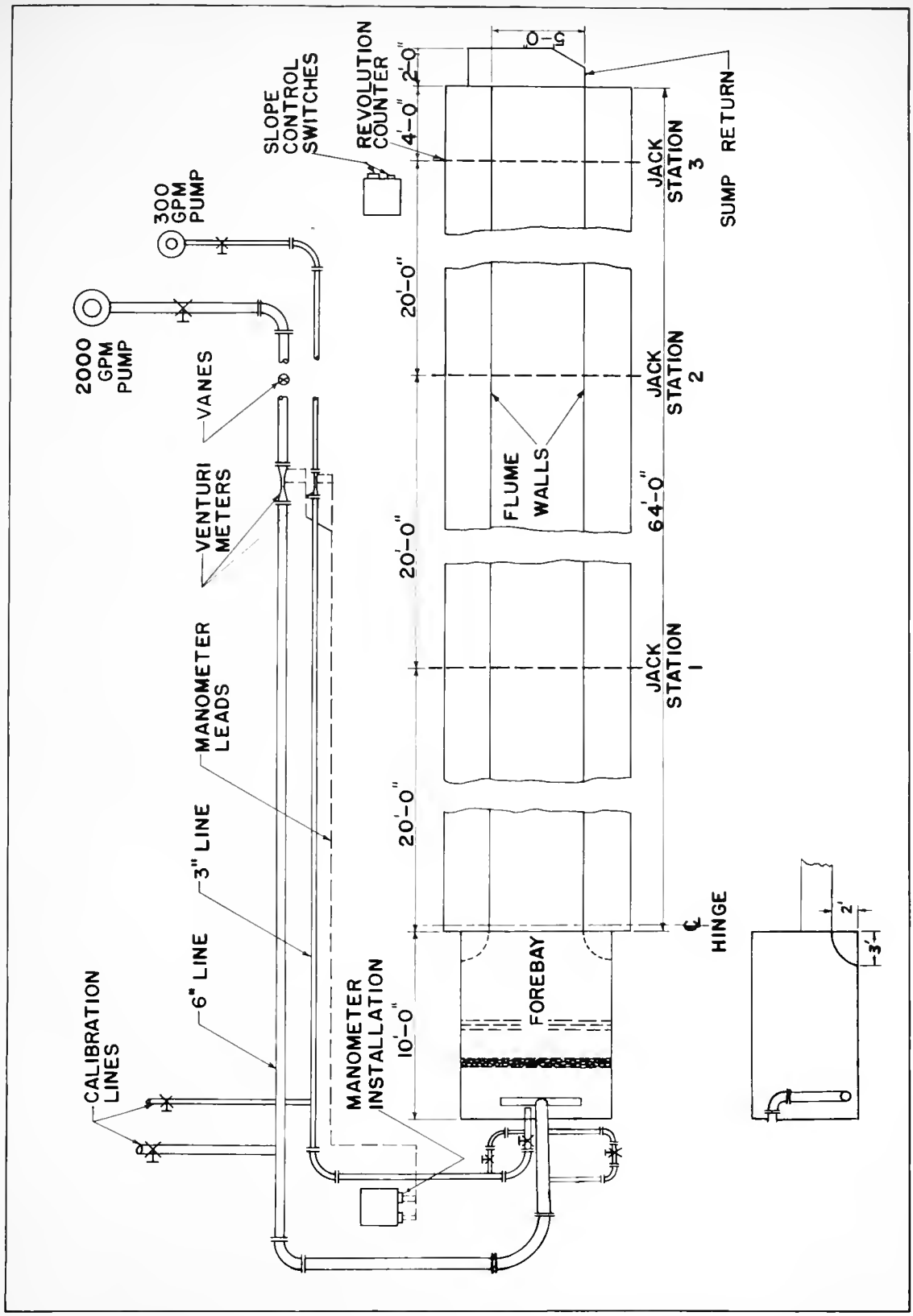

FIGURE 4 - APPARATUS ARRANGEMENT

FIG 5 MODELS

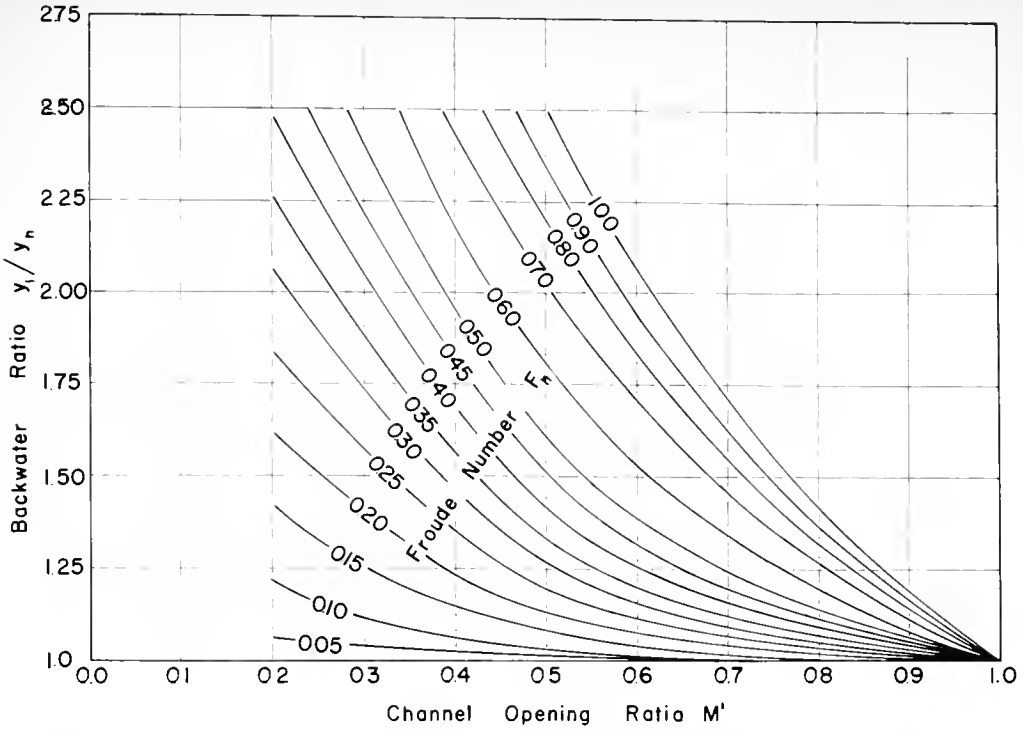

FIGURE 6a — BACKWATER RATIO VS CHANNEL OPENING RATIO L/b =0 SEMI-CIRC. SMOOTH CHANNEL

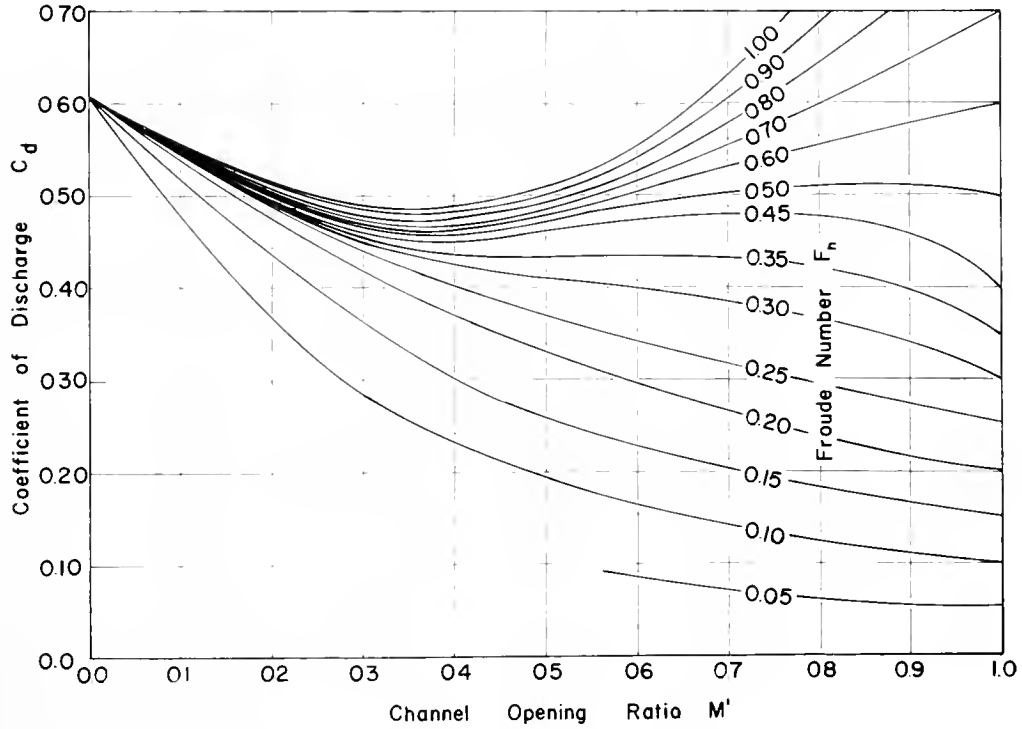

FIGURE 6b — DISCHARGE COEF. VS CHANNEL OPENING RATIO L/b =0 SEMI-CIRC SMOOTH CHANNEL

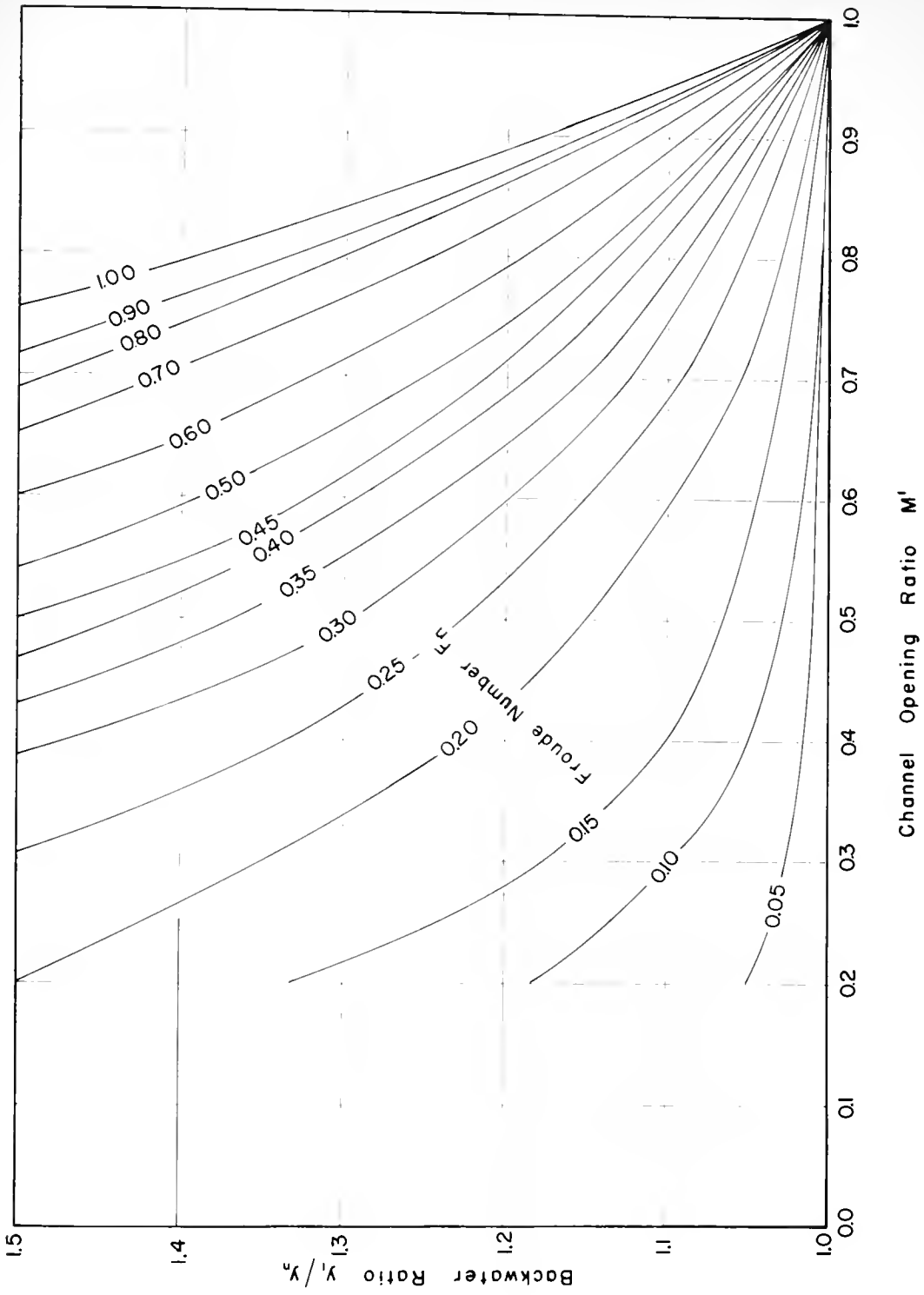

FIGURE 7a — BACKWATER RATIO VS CHANNEL OPENING RATIO L/b=0 SEMI-CIRC. ROUGH CHANNEL $y_1/y_n \leq 1.50$

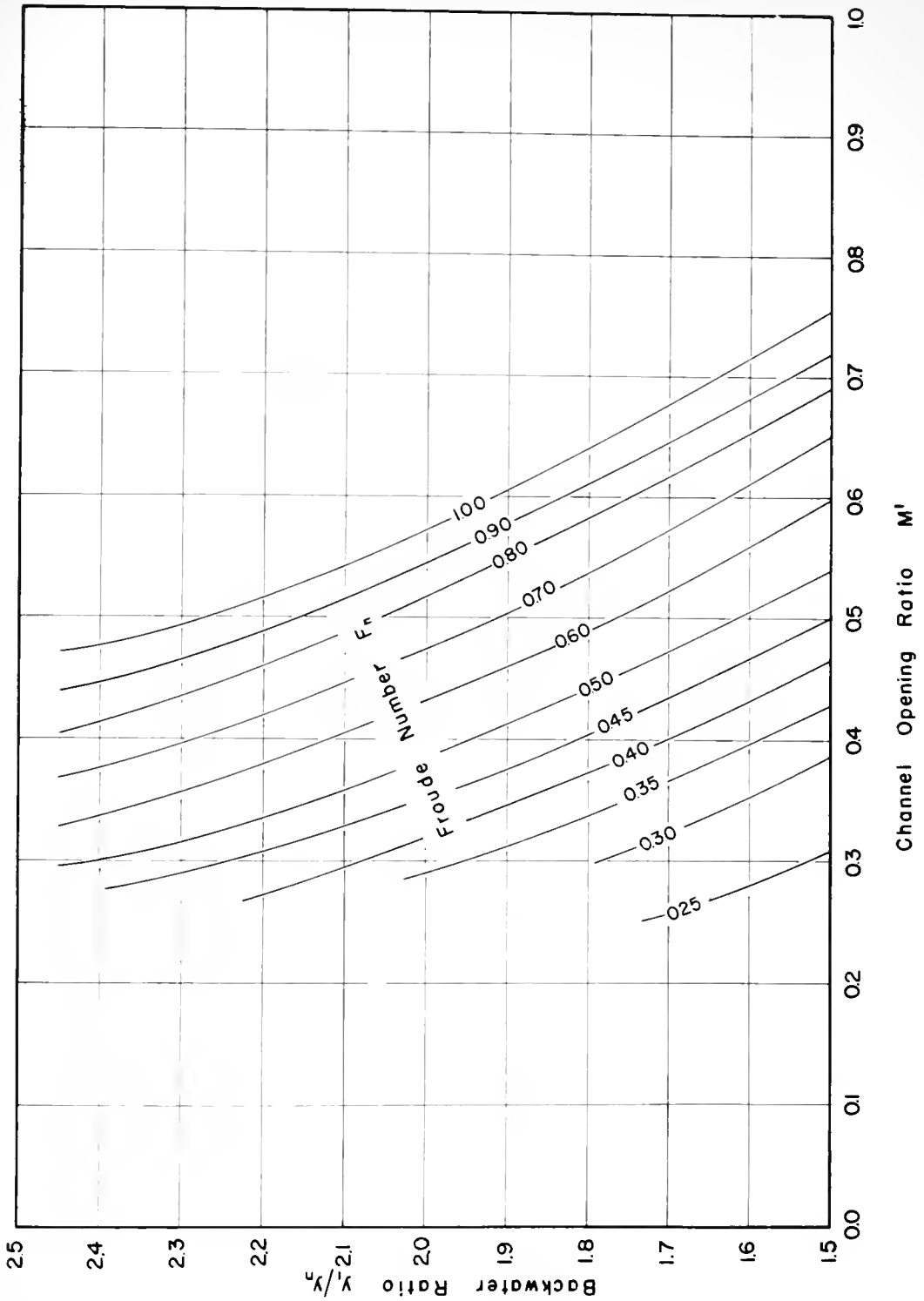

FIGURE 7b — BACKWATER RATIO VS CHANNEL OPENING RATIO L/b=0 SEMI-CIRC. ROUGH CHANNEL $1.50 \leqslant y_1/y_n \leqslant 2.50$

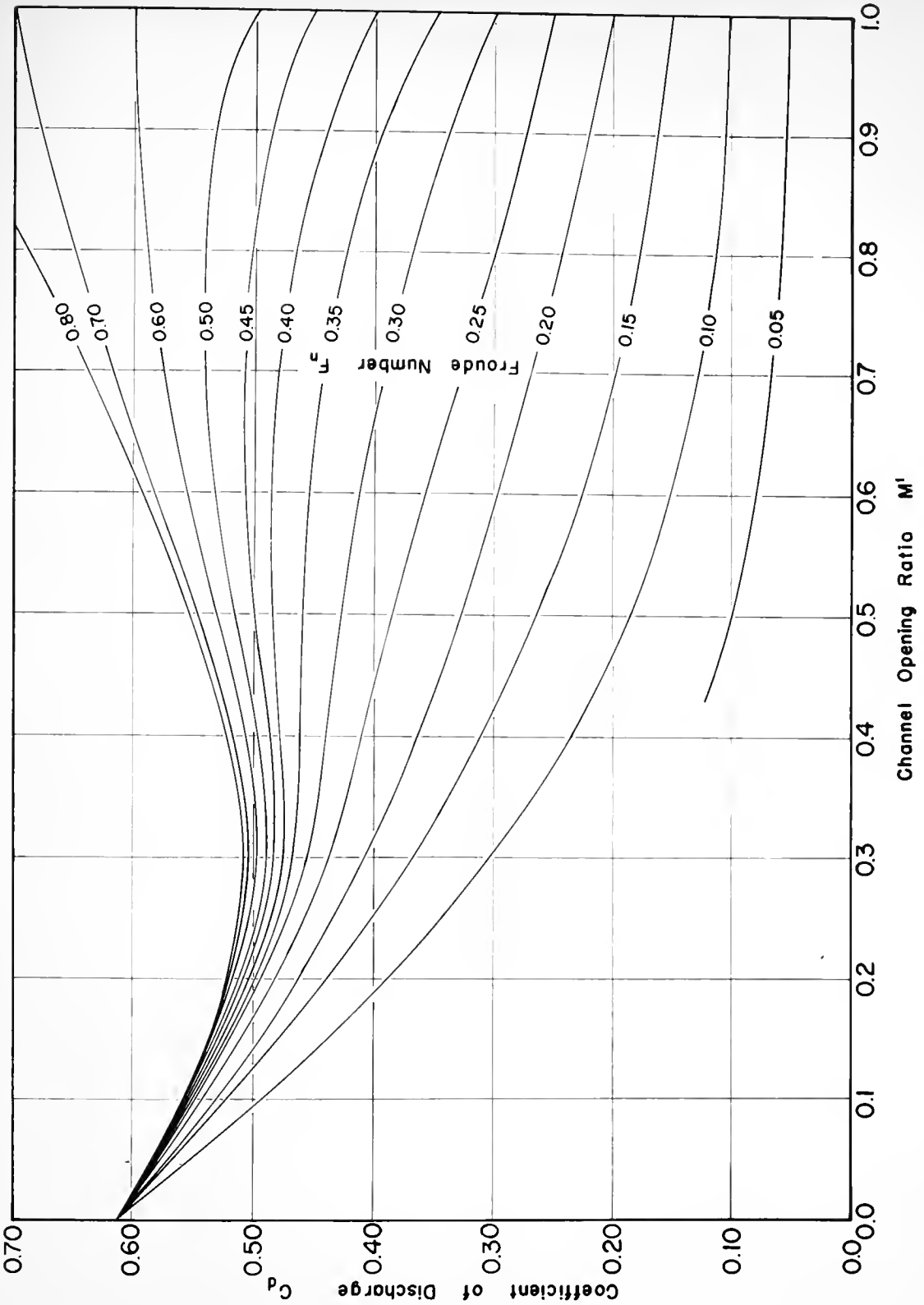

FIGURE 8 — DISCHARGE COEF. VS CHANNEL OPENING RATIO L/b=0 SEMI-CIRC. ROUGH CHANNEL

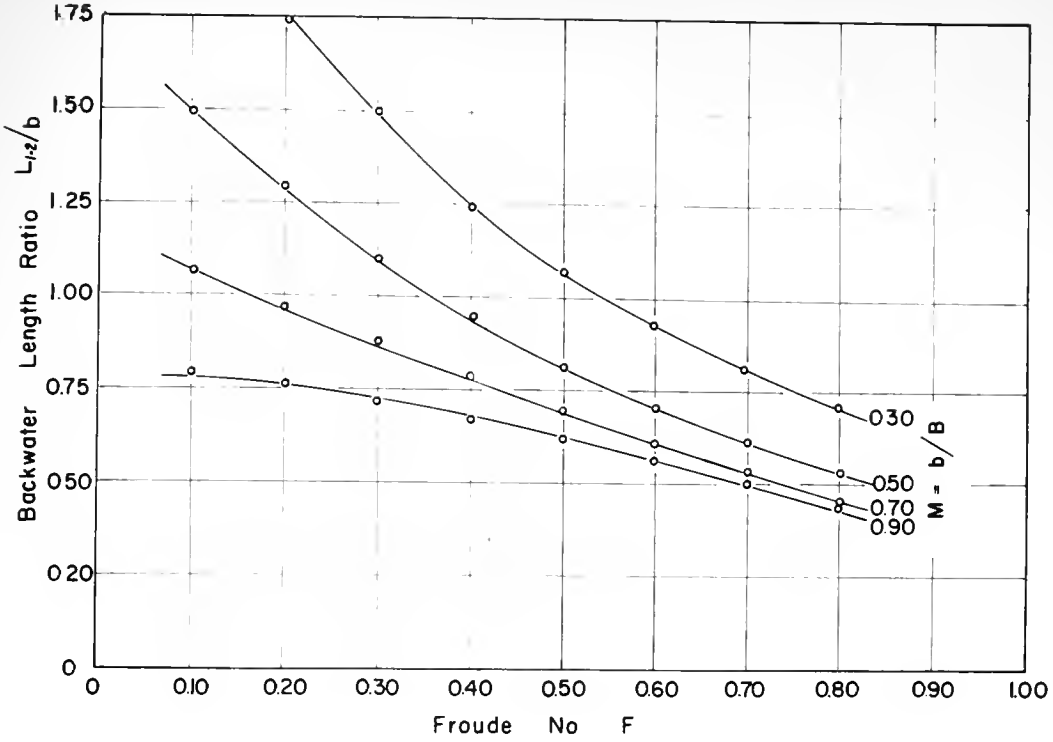

FIGURE 9a — LENGTH TO MAXIMUM BACKWATER

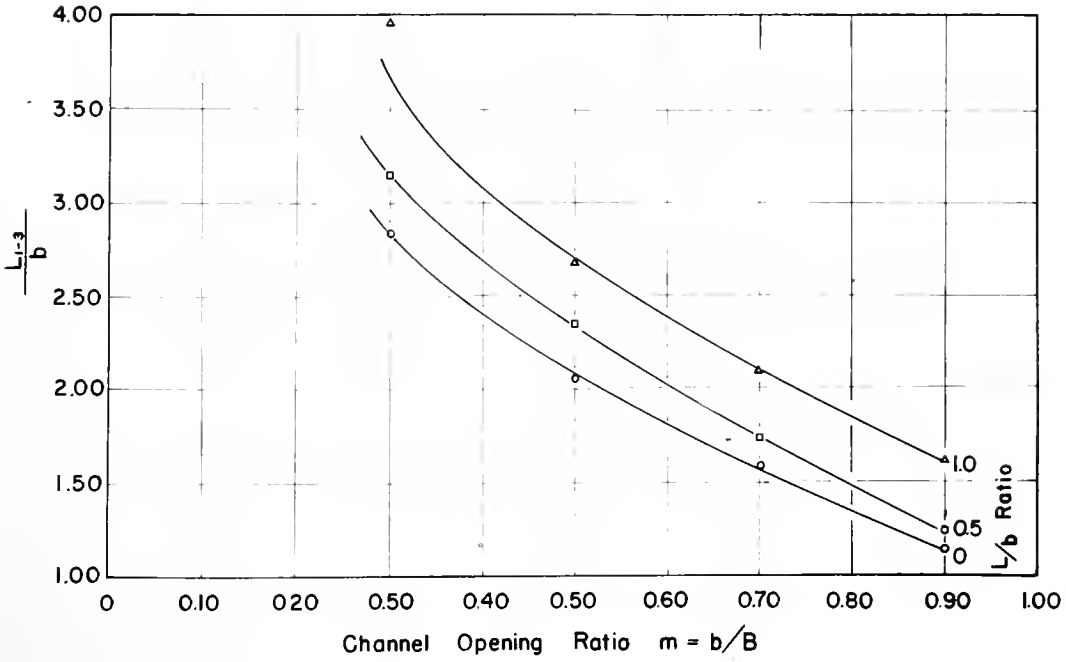

FIGURE 9b — LENGTH OF SURFACE PROFILE BETWEEN y_1 & y_3

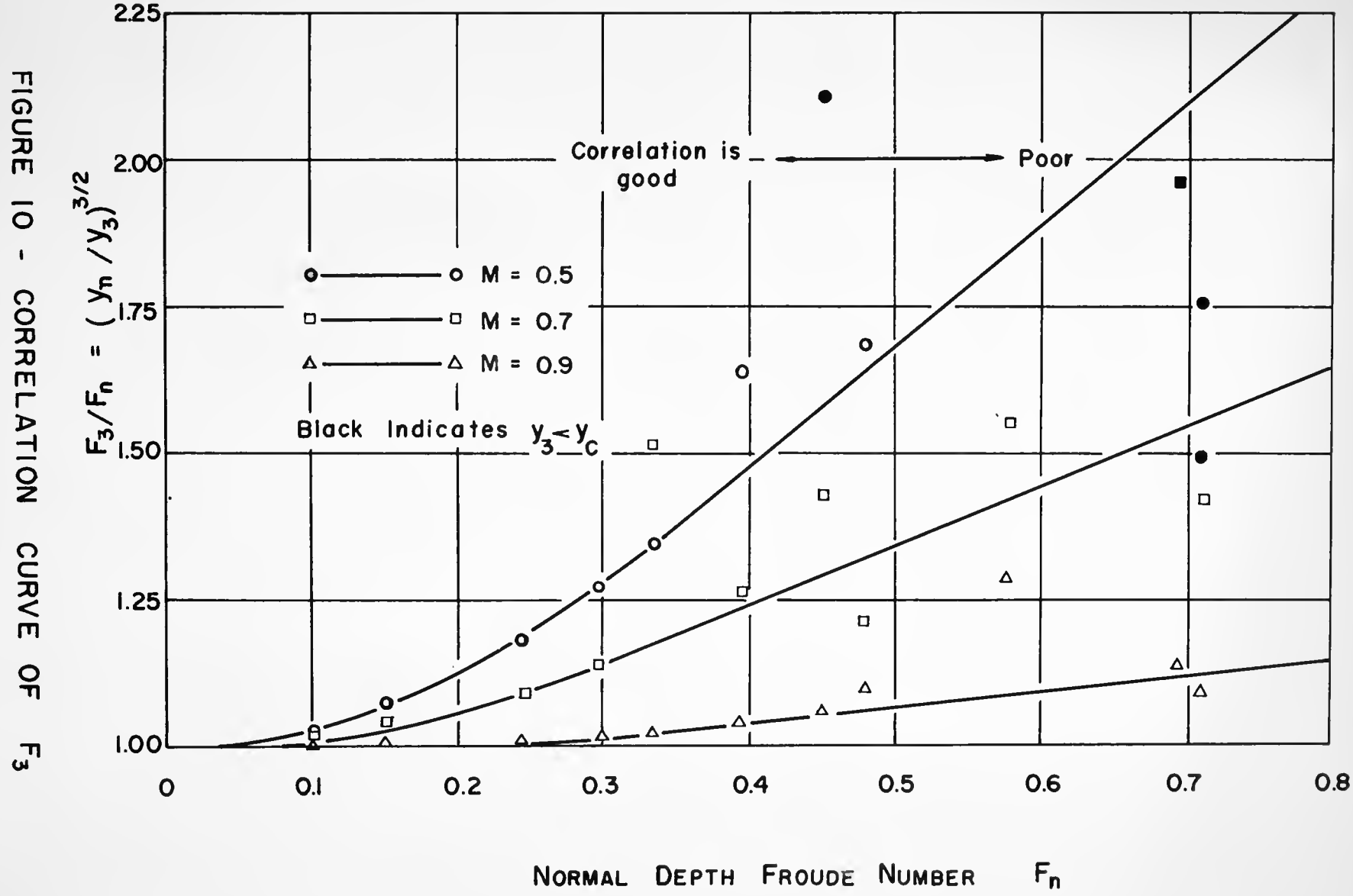

FIGURE 10 - CORRELATION CURVE OF F_3

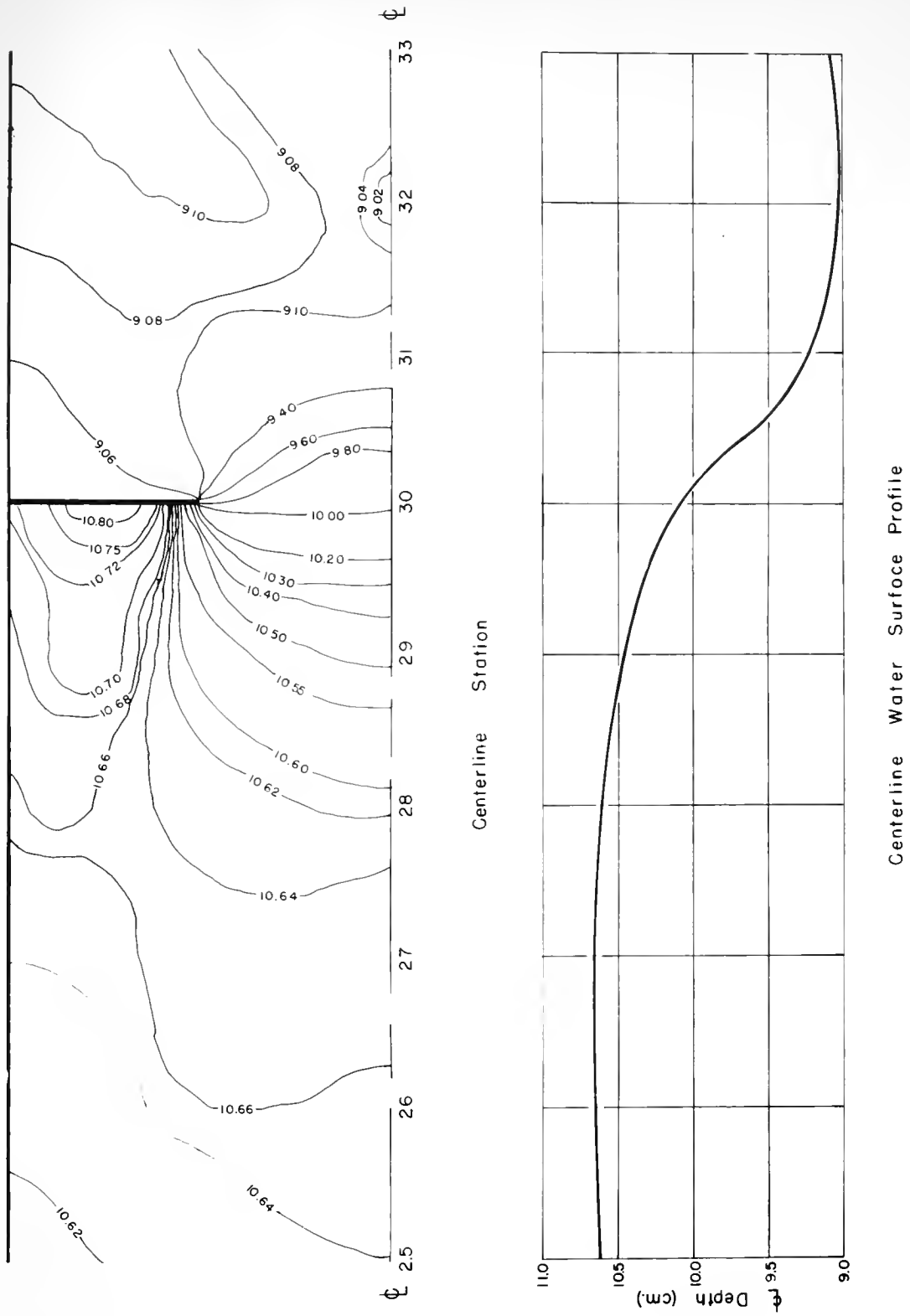

FIGURE 11 – SURFACE TOPOGRAPHY Q = 1 CFS,
S = 0.000584, M = 0.5, L/b = 0

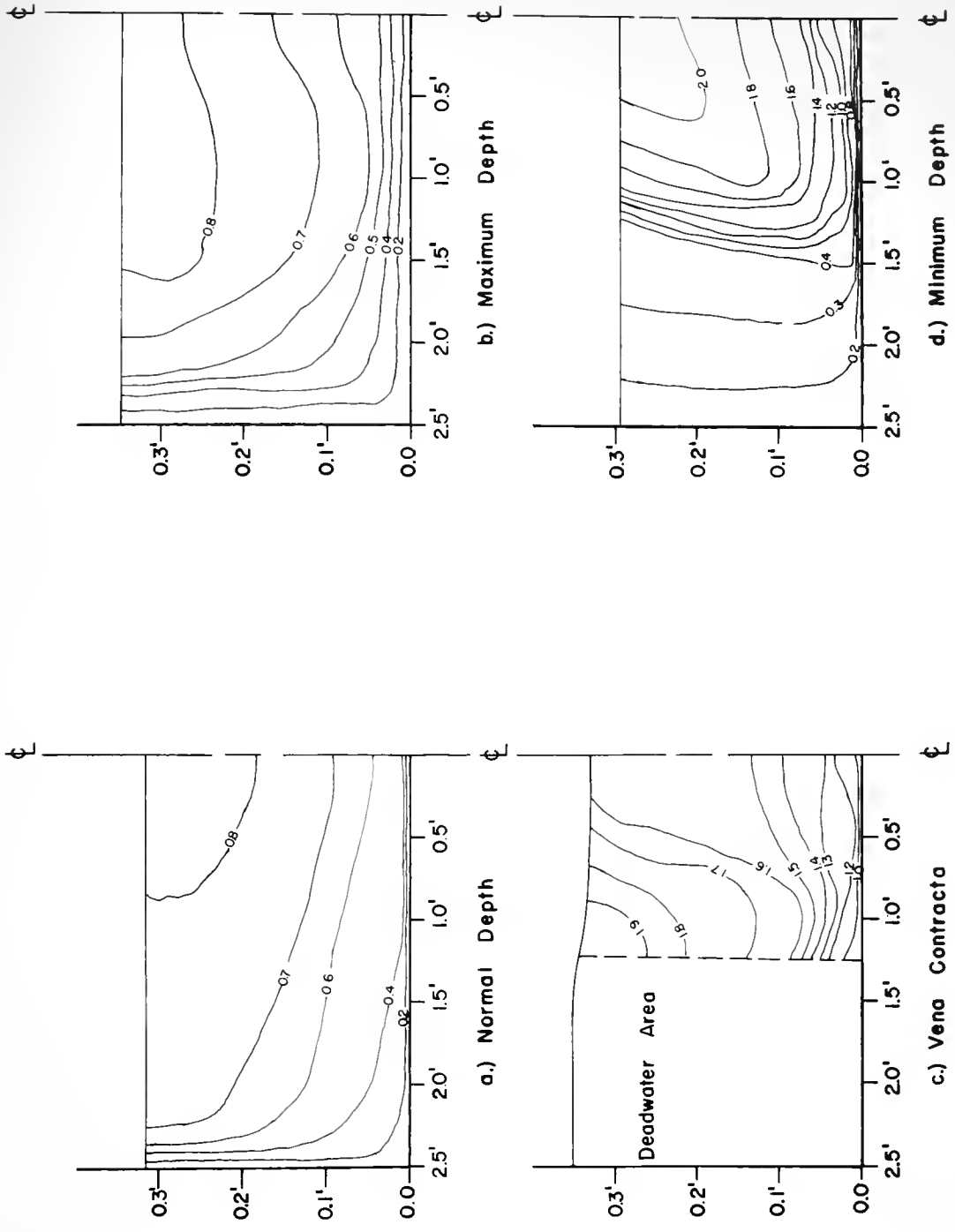

FIGURE 12 -ISOVEL DIAGRAMS IN FPS Q=1CFS,
S=0.000584, M=0.5, L/b=0

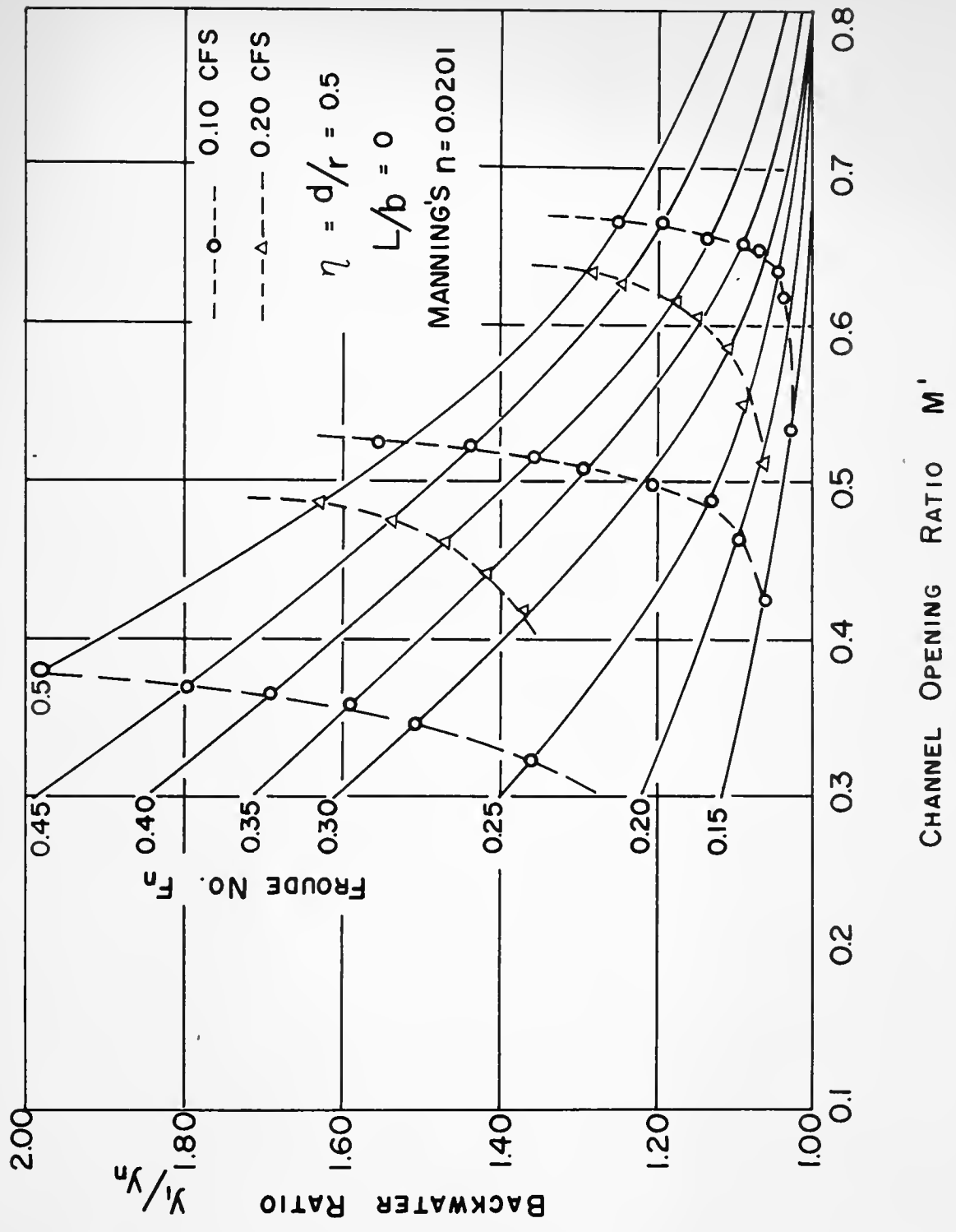

FIGURE 13- VARIATION OF THE BACKWATER RATIO FOR SEGMENT ARCHES SMALL FLUME - ROUGH BOUNDARIES

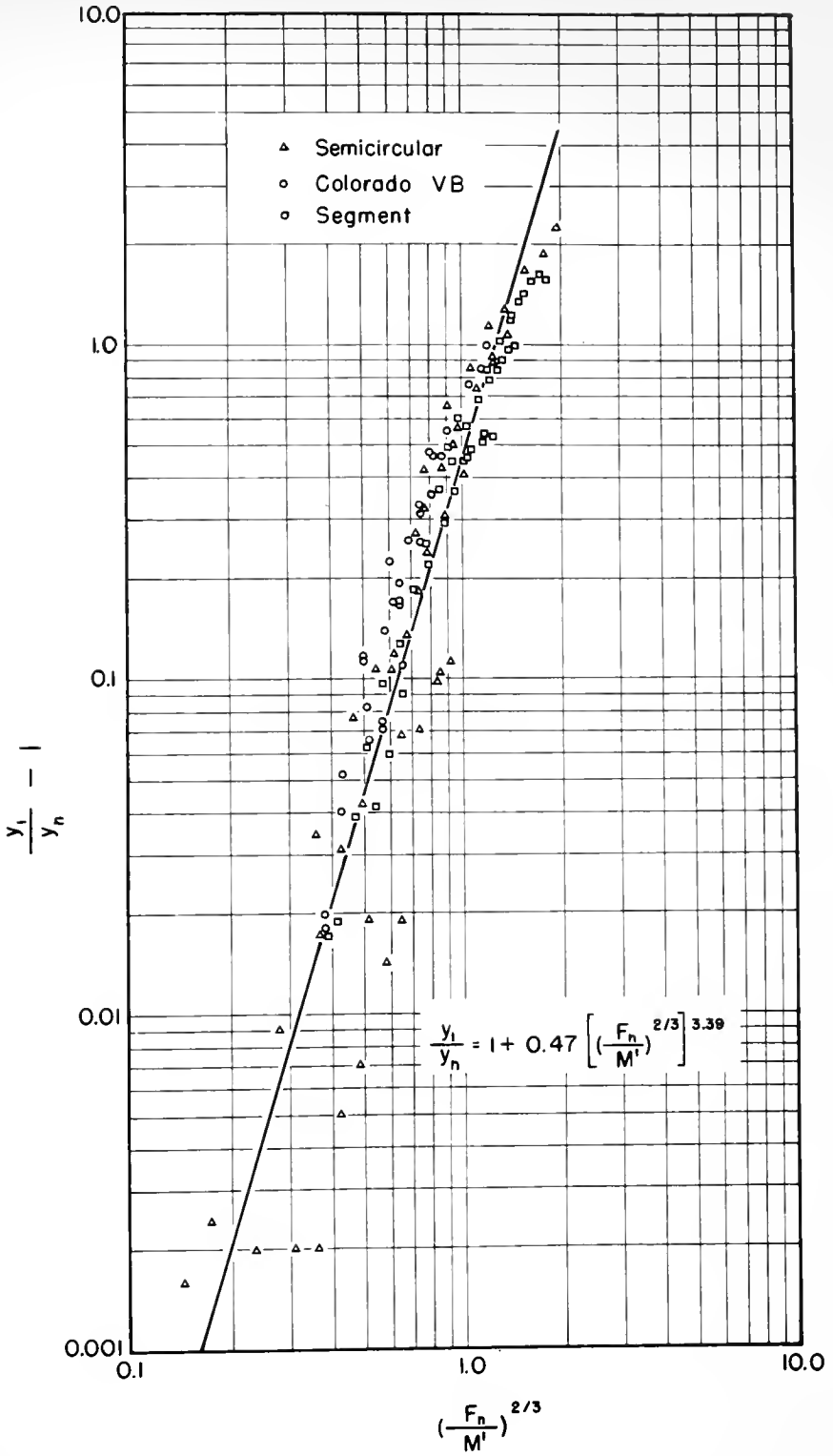

FIGURE 14 – GENERALIZED BACKWATER RATIO

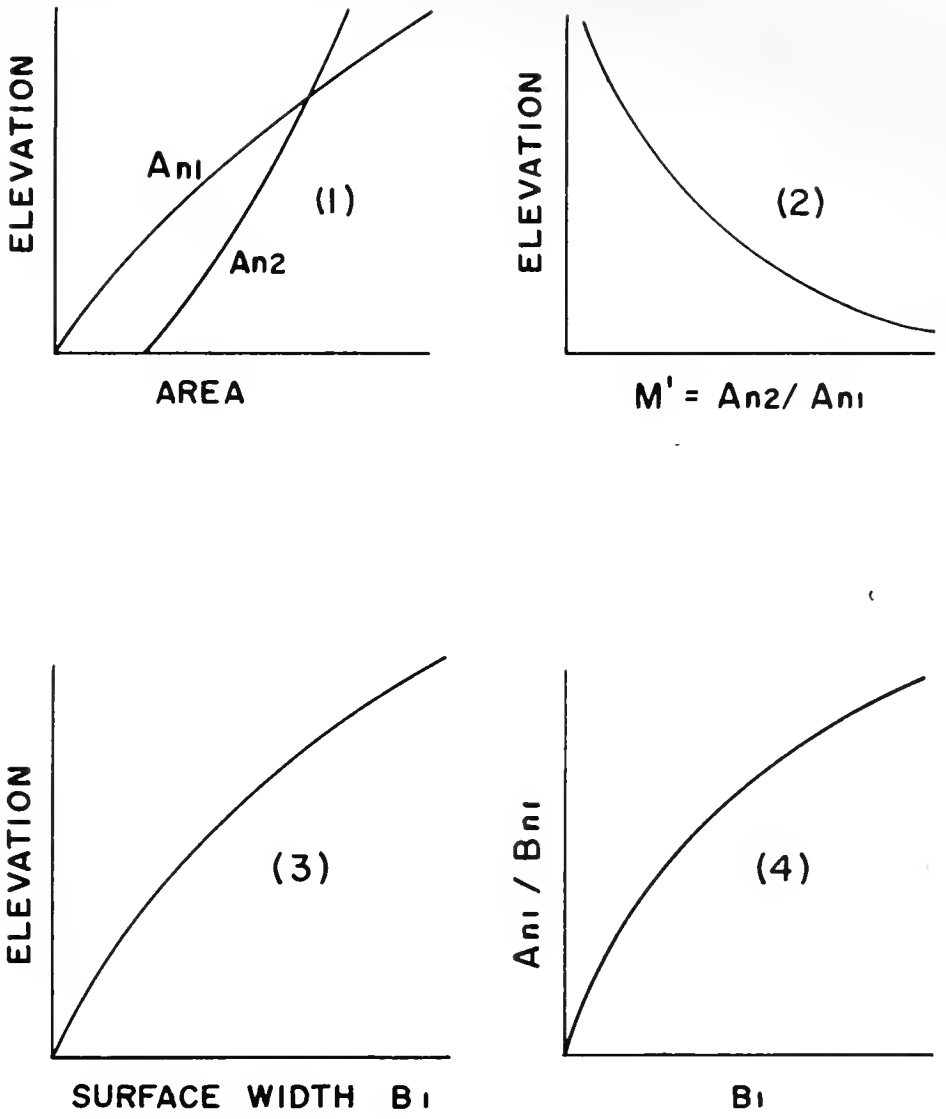

FIGURE 15 - WORKING CURVES FOR INDIRECT DISCHARGE MEASUREMENT